

Steam reforming of tar from a biomass gasification process over Ni/olivine catalyst using toluene as a model compound

D. Świerczyński, S. Libs, C. Courson*, A. Kiennemann

Laboratoire des Matériaux, Surfaces et Procédés pour la Catalyse, ECPM, UMR 7515, 25, rue Becquerel, 67087 Strasbourg Cedex 2, France

Received 21 September 2006; received in revised form 22 January 2007; accepted 29 January 2007

Available online 9 February 2007

Abstract

A Ni/olivine catalyst, previously developed for biomass gasification and tar removal during fluidized bed steam gasification of biomass, was tested in a fixed bed reactor in toluene steam reforming as a tar destruction model reaction. The influence of the catalyst preparation parameters (nickel precursor, calcination temperature and nickel content) and operating parameters (reaction temperature, steam to carbon S/C ratio and space-time) on activity and selectivity was examined showing a high toluene conversion and a low carbon formation compared to olivine alone. The steam reforming of toluene was found to be of zero order for water and first order for toluene. Activation energy required for Ni/olivine was determined to be about 196 kJ mol⁻¹ in accordance with literature. Catalyst activity and stability and its resistance against carbon formation were discussed on the basis of X-ray diffraction (XRD), transmission electron microscopy (TEM) and temperature programmed oxidation (TPO) results. Characterization before test (XRD, temperature programmed reduction (TPR), Mössbauer spectroscopy) have shown the presence of NiO–MgO solid solution, formed on the surface of olivine support, which explains the efficiency of the catalyst calcined at 1100 °C. After test, Ni–Fe alloys were observed (TEM, Mössbauer spectroscopy). It was suggested that magnesium oxide enhanced steam adsorption, facilitating the gasification of surface carbon and that Ni–Fe alloys prevented carbon deposition by dilution effect.

© 2007 Elsevier B.V. All rights reserved.

Keywords: Ni/olivine catalyst; Tar removal; Toluene steam reforming; Carbon formation

1. Introduction

Since the constant increase in petroleum price, use of biomass as a partial replacement for fossil fuels via biomass to liquid (BTL) or biomass to gas (BTG) processes is more and more intended. The value of biomass can be increased via thermal, biological or physical processes. Thermochemical conversion technologies are especially useful to produce fuels, chemicals, combined heat and power with high-energy efficiencies. Among them, biomass gasification has attracted a lot of interest by producing a gas rich in CO and H₂ used for methanol or Fischer-Tropsch synthesis, chemicals production or electricity generation (turbine, gas engine or fuel cells). Previous studies, in pilot [1] as well as in demonstration scale [2], have demonstrated that biomass steam gasification, in the dual fluidized bed gasifier (fast internally circulating

fluidized bed gasifier: FICFB), was an efficient process used to produce a nearly nitrogen-free (<2%), hydrogen-rich product gas.

However, one of the most crucial problems in biomass gasification technology [3] is the removal of tar, which is a mixture of condensable aromatic compounds [4]. Tar can condense or polymerize into more complex structures in exit pipes, heat exchangers or on particulate filters, leading to choking and attrition. This can result in a decrease of total efficiency and an increase in the cost of the process. Tar elimination from the gasification product is necessary before additional usage in any application.

Tar removal technologies can be divided into two approaches: hot gas cleaning after the gasifier (secondary methods), and treatments inside the gasifier (primary methods). The secondary methods include tar cracking, either thermally or catalytically, or mechanical separation using cyclones, filters or scrubbers. Although these methods have proven to be effective, treatments inside the gasifier are gaining more attention as they may eliminate the need for downstream

* Corresponding author. Tel.: +33 390 2427 70; fax: +33 390 2427 68.

E-mail address: coursonc@ecpm.u-strasbg.fr (C. Courson).

cleanup. The different approaches of primary treatment are: (a) proper selection of operating parameters, (b) use of bed additive/catalyst and (c) gasifier modifications [5].

For both secondary and primary methods, the catalytic steam reforming process is a very attractive technique for tar destruction [4]. Calcined dolomites are the most widely used non-metallic catalysts for tar conversion [6–15], but their low attrition resistance renders them inappropriate for use in fluidized bed reactors. An effective solution for tar reforming was proposed by Corella [16], consisting of a calcined dolomite guard bed to decrease tar content, followed by a fixed bed Ni catalyst reforming reactor operating at about 800 °C. Olivine, another naturally occurring mineral, has demonstrated activity in tar conversion similar to that of calcined dolomite [15,17]. Its advantage, in comparison with dolomite, is a high attrition resistance, allowing its direct use as a primary catalyst in fluidized bed gasifiers.

Ni catalysts have been used extensively for biomass gasification tar conversion [12,16,18–21] because of their high tar destruction activity, along with the added advantages of methane reforming and water gas shift activity, allowing adjustment of the H₂/CO ratio of the product gas. Some studies [22,23] have also shown that nickel catalyzes the reverse ammonia reaction, reducing the amount of NH₃ in gasification product gas. This is particularly important if it is used in a gas turbine, as NO_x can be formed easily from NH₃.

Two main limitations for Ni catalysts should be stressed. Because of the attrition phenomena in fluidized bed reactors, the use of Ni catalysts was generally as a secondary catalyst in separate fixed bed reactors, although recently some authors have developed or studied nickel catalysts for fluidized bed use [24–28]. The second limitation of nickel catalysts is the rapid deactivation, caused by carbon formation on the catalyst surface. This can be substantial when the tar level in the product gas is high.

Previously, a Ni/olivine catalyst was developed [29,30], characterized [31,32] and used in the FICFB gasifier as a primary catalyst showing activity in tar destruction and methane reforming [33]. To understand better the parameters influencing its activity, a study using simplified model conditions was required. Toluene was used as a model tar compound as it represents a stable aromatic structure found in tar formed during high-temperature processes [4].

The goal of the present work was to demonstrate the efficiency of a Ni/olivine catalyst for tar reforming, as well as its resistance to deactivation by carbon deposition in a fixed bed laboratory reactor. The efficacy of catalyst was tested as a function of different preparation parameters (calcination temperature, nickel precursor) and different operating conditions (reaction temperature, S/C ratio and space-time). Kinetic parameters were evaluated for the optimized catalytic system and special attention was paid to catalyst stability, especially stability linked to carbon formation.

2. Experimental

2.1. Catalyst preparation

2.1.1. Olivine support

Natural olivine was acquired from an Austrian mine (Magnolithe GmbH). It was delivered after calcination at 1600 °C over 4 h, followed by crushing and sieving to obtain particle sizes between 400 and 600 μm. This olivine will be referred to initial olivine. Its composition (30.5 wt% of Mg, 7.1 wt% of Fe and 19.6 wt% of Si), obtained by atomic absorption (CNRS Centre in Vernaison), resulted in the mean global formula (Mg_{0.94}Fe_{0.01})₂SiO₄ (without taking into account the minority elements: Ni, Ca, Al, Cr, lower than 0.2 wt% each). In fact, as shown in [34], natural olivine contains mainly the phase of (Mg_{0.94}Fe_{0.06})₂SiO₄ with small quantities of its oxidation products: MgSiO₃, and iron oxides (~3 wt% of iron in the form of MgFe₂O₄ and probably α-Fe₂O₃). The specific surface area of olivine is very low (<1 m² g⁻¹). Reducibility of this initial olivine calcined in the same conditions as the Ni/olivine catalyst was described previously [34].

2.1.2. Ni/olivine catalyst

In order to study the effect of the preparation parameters, a series of Ni/olivine catalysts were synthesized with various nickel precursors and contents, and calcined at different temperatures. Ni/olivine catalysts were prepared by wet impregnation of initial olivine using an excess of nickel salt (nitrate, chloride or acetate) aqueous solution. After solvent evaporation, the sample was dried overnight at 100 °C and calcined at various temperatures (400, 900, 1100 or 1400 °C) over 4 h, using a temperature increase slope of 3 °C min⁻¹. The concentration of the nickel nitrate solution was modified in order to obtain catalysts containing from 1.5 to 5.7 wt% of nickel after calcination at 1100 °C [30].

The different preparation ways resulted in the series of Ni/olivine catalysts described in Table 1.

2.2. Steam reforming of toluene (SRT)

2.2.1. Experimental bench and operating conditions

The scheme of the experimental bench used for toluene steam reforming is shown in Fig. 1. Experiments were carried out at atmospheric pressure in a fixed bed quartz reactor (6.6 mm i.d.) placed in a furnace. The catalyst bed was held by quartz wool in the uniform temperature zone. The temperature was monitored by a thermocouple placed outside of the reactor near the catalyst bed. The furnace temperature was controlled with a Microcor III PR temperature controller. The catalyst was initially activated under the reactants gas mixture during 30 min at 750 °C and then tested for 7 h at a given temperature. The temperature range (560–850 °C) of the experiments was chosen to cover all possible conditions that may occur in practice in the FICFB gasifier.

For the feed gas mixture, argon was used as a diluent gas. Its flow was regulated by mass flowmeter. Water and toluene were introduced by syringe pumps into a vaporization furnace (120 °C), and then carried to the reactor by argon flow.

Table 1

Ni/olivine catalysts synthesized for the study of preparation parameter effects and their estimated wt% of metallic iron and nickel after reduction and by TPR

Sample	Nickel salt	Calcination temperature (°C)	Nickel content (wt%)		Reduced metal (wt%)	
			Theoretical	Real	Fe ⁰ ^a	Ni ⁰ ^b
N1100	Nitrate	1100	3.9	3.9	2.4	1.3
C1100	Chloride	1100	3.9	3.8	–	–
A1100	Acetate	1100	3.9	2.7	–	–
N400	Nitrate	400	3.9	3.9	1.4*	2.2
N900	Nitrate	900	3.9	3.9	1.6*	2.2
N1400	Nitrate	1400	3.9	3.9	3.8	0
1.5%N1100	Nitrate	1100	1.6	1.5	2.4	–
5.7%N1100	Nitrate	1100	7.9	5.7	2.4	5.3

^a The quantity of reduced Fe⁰ was estimated on the base of Mössbauer spectra with exception of the samples marked by asterisk, for which the estimation was made from TPR results of olivine calcined at the same temperature with the hypothesis that all the H₂ consumption is due to Fe³⁺ to Fe⁰ reduction.

^b The quantity of reduced nickel was estimated by the difference between H₂ consumption measured by TPR of the corresponding Ni/Olivine sample and that needed for the reduction of iron.

Based on literature data concerning the amount of tar produced during biomass steam gasification [35], toluene concentration in argon was fixed at 27 g Nm⁻³ (0.7 vol.%) in order to perform catalytic tests under more sever conditions than in the FICFB gasifier.

To study operating parameters effects, 200 mg of catalyst was used and the feed mixture at 25 °C contained 45 mL min⁻¹ of Ar, 2.8–8.8 mL min⁻¹ of H₂O (g) (S/C molar ratio varied from 1.1 to 3.4) and 0.37 mL min⁻¹ of toluene (g), corresponding to a space-time at 25 °C ($w_{\text{cat}}/F_{\text{toluene}}$) of 9 kg_{cat} h m⁻³.

For determination of kinetic parameters, operating conditions were the following:

- total feed flow rate at 25 °C: 0.0156 m³ h⁻¹;
- gas volumes composition: 92% of Ar, 7.5% of H₂O and 4709 ppm of toluene (toluene feed flow rate at 25 °C (F_{toluene}): 6.7 × 10⁻⁵ m³ h⁻¹);
- S/C molar ratio: 2.3;
- catalyst amount (w_{cat}) included between 5 and 300 mg, corresponding to a space-time at 25 °C ($w_{\text{cat}}/F_{\text{toluene}}$) between 7 × 10⁻² and 4.48 kg_{cat} h m⁻³.

2.2.2. Products detection and quantification

The resultant gas stream was analyzed simultaneously by three on-line gas chromatographs. The product gases (CH₄, CO₂, CO, H₂) were analyzed by two chromatographs, equipped

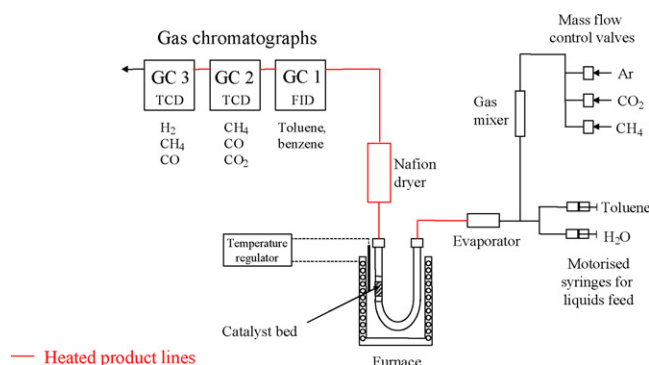


Fig. 1. Experimental set-up for toluene steam reforming.

with a thermal conductivity detector (TCD). The first quantified CH₄, CO₂ and CO separated on a packed carbosieve SII column (3 m; 80–100 mesh; He 25 mL min⁻¹), and the second determined quantities of CO and H₂ separated on molecular sieves (5 Å; 2 m; 80–100 mesh; Ar 18 mL min⁻¹). The third, a Varian 3400 CX equipped with a flame ionization detector, determined the quantities of toluene, benzene and heavier aromatic products by separation on a HP-5 (0.53 mm × 30 m) capillary column.

Selectivity towards carbon formed on the catalyst surface represented at 560 and 800 °C, respectively 1.4% and <0.1% of all carbon converted during test period. Carbon formation was not taken into account in carbon balance calculations. Consequently the conversions, yields and selectivities were calculated with the formulae shown below.

Toluene conversion, noted X_c (Eq. (1)), is the ratio of the carbon present in toluene converted into carbon-containing gas products (CO, CO₂, CH₄ and C₆H₆).

$$X_c(\%) = \frac{[\text{CO}]_{\text{out}} + [\text{CO}_2]_{\text{out}} + [\text{CH}_4]_{\text{out}} + [\text{C}_6\text{H}_6]_{\text{out}}}{7[\text{T}]_{\text{in}}} \times 100 \quad (1)$$

[T]: toluene molar concentration.

Hydrogen yield, noted Y_{H_2} (Eq. (2)), is expressed as the percentage of the stoichiometric potential corresponding to the total conversion of toluene into H₂ and CO₂ according to the reaction (5) developed further in the results section.

$$Y_{\text{H}_2}(\%) = \frac{[\text{H}_2]_{\text{out}}}{8[\text{T}]_{\text{in}}} \times 100 \quad (2)$$

Selectivities of carbon containing products, noted S_i (Eq. (3)), are defined as the ratio of the amount of carbon in the product i to the amount of carbon in the reacting toluene.

$$S_i(\%) = \frac{[i]_{\text{out}}}{7\{[\text{T}]_{\text{in}} - [\text{T}]_{\text{out}}\}} \times 100$$

[i]: molar concentration $i = \text{CO}, \text{CO}_2, \text{CH}_4, \text{C}_6\text{H}_6$

(3)

2.3. Characterization techniques for catalysts after SRT

2.3.1. X-ray diffraction (XRD)

Samples were characterized by powder X-ray diffraction (XRD) on a Siemens D500TT diffractometer using Cu K α radiation in order to identify the potential evolution of the crystalline phases during SRT tests. The diffractograms were registered in the range of 2θ between 20° and 90° with a step of 0.05° and a step time of 6 s.

2.3.2. Temperature programmed reduction (TPR)

To quantify the amount of reducible iron and nickel, the reducibility of the catalyst has been followed by temperature-programmed reduction (TPR) performed on 200 mg of catalyst placed in a U-shaped quartz tube (6.6 mm i.d.). The reducing gas mixture ($H_2 = 0.12 \text{ L h}^{-1}$ and $Ar = 3 \text{ L h}^{-1}$) passed through the reactor heated from room temperature to 950°C with a slope of $15^\circ\text{C min}^{-1}$ then maintained at 950°C until the end of H_2 consumption showed by the baseline return. A thermal conductivity detector (TCD) was used for quantitative determination of hydrogen consumption.

2.3.3. Mössbauer spectroscopy

The ^{57}Fe Mössbauer spectra were recorded at -196°C (77 K) using a spectrometer with a triangular waveform and a ^{57}Co source (50 mCi) dispersed in a rhodium matrix. From the obtained spectra, the isomeric shifts were determined in comparison with a metallic iron standard at room temperature. To identify different forms of iron present in the sample, the spectra were fitted using the MossFit computer program.

2.3.4. Transmission electron microscopy (TEM)

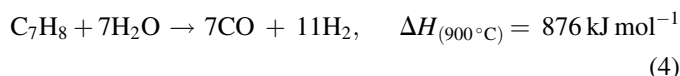
Transmission electron microscopy (TEM) was performed on a Topcon EM 002B apparatus coupled to energy dispersive X-ray spectroscopy (EDXS). The samples were grounded in a mortar, and subsequently deposited on a Cu grid covered with a perforated carbon membrane. Microanalysis was used to reveal the new phases formed during SRT tests.

2.3.5. Temperature programmed oxidation (TPO)

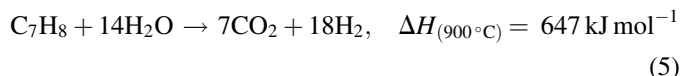
Temperature programmed oxidation (TPO) is a procedure that allows exposure of a sample to a gaseous flow of oxygen diluted in an inert gas during an increase in temperature. This technique detects the presence of different oxidizable species (different carbon forms) by differences in their oxidation temperatures and rates. CO_2 , CO and H_2O formed and O_2 consumed are quantified versus temperature by a mass spectrometer (quadrupole—Fisons Instruments). The amount of carbon deposit oxidized during the analysis was deducted from the amount of carbon-containing products (CO_2). After SRT tests, TPO analysis was performed with 25 mg of catalyst placed in a similar reactor than that used for SRT tests. The oxidizing gaseous mixture ($\text{O}_2 = 5 \text{ mL min}^{-1}$ and $\text{He} = 45 \text{ mL min}^{-1}$) was passed through the reactor heated from room temperature to 950°C ($15^\circ\text{C min}^{-1}$). A mass spectrometer calibration was performed previously with a known amount of CO_2 .

3. Results and discussion

Because of the complexity of the gasification gas product, many parallel and consecutive reactions can take place during hot gas cleaning. In order to simplify the model we hypothesized that toluene reacted principally with water to produce hydrogen and carbon monoxide (Eq. (4)):

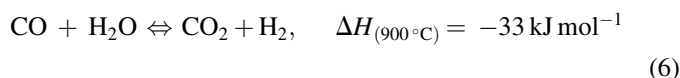


or hydrogen and carbon dioxide (Eq. (5)):



These reactions become thermodynamically possible above 435 and 350°C , respectively.

In fact, the water gas shift (WGS) reaction takes place simultaneously (Eq. (6)):

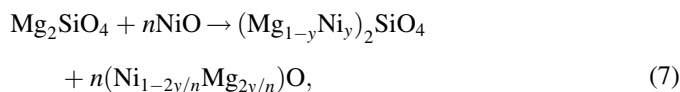


Other reactions have to be taken into account during steam reforming, such as carbon formation reactions by toluene decomposition and by CO dismutation (Boudouard). Boudouard reaction, the principal carbon formation reaction, is thermodynamically favored below 650°C .

3.1. Preparation parameters effect (choice of Ni precursor, Ni content and calcination temperature)

3.1.1. Summary of the catalyst characterization

As we have demonstrated in previous works [31,32], independently of the precursor salt and nickel content, the calcination of Ni/olivine systems leads to a reaction between the olivine main phase (for simplicity the Fe present in olivine is not indicated) and NiO according to:



where $n \leq 2$

Depending on the calcination temperature (400 – 1400°C), three states of the system can be distinguished [30]:

- after calcination at 400°C , a shell of free NiO was present on the olivine surface,
- after calcination at 1100°C , a few microns thick shell of NiO–MgO solid solution was formed on the olivine grain; calcination at temperatures higher than 1100°C led to the gradual diffusion of nickel into the bulk of olivine, and
- after calcination at 1400°C , nickel is fully integrated in the olivine structure ($y = n$ in the Eq. (7)).

These three states of the system showed different reducibility during TPR study (Fig. 2):

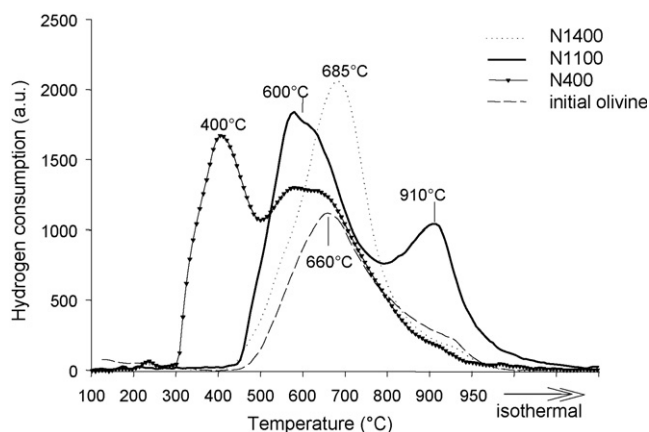


Fig. 2. TPR profiles for the initial olivine and N400, N1100 and N1400.

- after calcination at 400 °C, free NiO was reducible at ~400 °C,
- after calcination at 1100 °C, there was no more NiO reduction peak at ~400 °C and the NiO–MgO solid solution was reducible at ~910 °C [36], and
- after calcination at 1400 °C, nickel species became totally irreducible in the conditions of TPR.

Additionally to the reduction of Ni species, reduction of Fe species from the olivine support has mainly contributed to the reduction zones with maximum changing from 600 to 685 °C, depending of the calcination temperature (Fig. 2).

3.1.2. Evaluation of the amount and the size of reduced Ni and Fe species

As shown previously, the reduction of Ni species occurs in a wide range of temperatures from 400 up to 900 °C and superposes with reduction of Fe species of the olivine [30,31]. For this reason it is impossible to quantify the reduced neither Ni nor Fe species only based on the TPR of Ni/olivine catalyst. Mössbauer study of the reduced catalysts N1100, 1.5%N1100, 5.7%N1100 and N1400 has permitted to quantify the reduced iron. For these samples the reduced nickel estimation was obtained by the difference between H₂ consumptions measured by TPR of the corresponding sample and that needed for the reduction of iron quantified by Mössbauer spectroscopy (Table 1).

On the other hand, characterization of the reduced N1100 catalyst by Mössbauer spectroscopy have permitted to verify that the quantity of reduced iron in Ni/olivine catalyst [32] is similar to this in the olivine calcined at the same temperature [34]. Supposing this is true for other calcination temperatures, Table 1 presents an estimation of the quantity of Ni metal in the sample N400 and N900, calculated from the difference in H₂ consumption by TPR between Ni/olivine and olivine calcined at the same temperature.

Mean size of metallic particles calculated from the XRD peak widening of the main reflection for Ni (or Ni–Fe alloy kamacite) at 44.6 (2θ) was about 20 nm.

3.1.3. Nickel precursor effect

Nitrate, chloride and acetate were chosen as nickel precursors. The results obtained in steam toluene reforming

Table 2

Effect of nickel precursor, calcination temperature and nickel content on toluene conversion during steam reforming (at 800 °C; S/C = 2.3; time on stream = 6 h)

Sample	Toluene conversion (%)
N1100	99 ^a
C1100	48 ^a
A1100	82 ^a
N900	99 ^b
N1100	62 ^b
N1400	24 ^b
1.5%N1100	60 ^b
3.9%N1100	62 ^b
5.7%N1100	59 ^b

^a At a constant catalyst amount of 200 mg.

^b At a constant nickel amount of 0.3 mg.

at 800 °C, with a S/C ratio of 2.3 (Table 2), confirmed those obtained in dry reforming of methane [30]; the best activity was obtained with the catalyst prepared from nickel nitrate (N1100). For acetate (A1100), lower activity is probably related to lower impregnation efficiency related to the lower solubility of this salt in water, and thus resulting in lower real nickel content (Table 1). However, in the case of chloride precursor (C1100), the near 50% decrease of activity can be related to the presence of chlorides not totally evacuated during calcination of this sample.

3.1.4. Calcination temperature effect

The effect of calcination temperature (900, 1100 and 1400 °C) has been studied for the samples containing 3.9 wt% of Ni and obtained from nickel nitrate (Table 2). The catalytic tests were carried out at 800 °C for a S/C ratio of 2.3 and a catalyst mass (*w_{cat}*) of 7.7 mg. As previously observed in dry reforming of methane [30], catalytic activity decreased with increasing calcination temperature. This can be explained by graduate integration of nickel in the support structure. The catalyst calcined at 900 °C (N900) was the most active of the series (99% of toluene conversion), presenting also the highest Ni reduction degree (2.2 wt% of Ni⁰). However, as previously shown by TPR studies, this system contained free nickel (nickel reducible at low temperature ~400 °C) that facilitates carbon deposition and leads to catalyst deactivation (toluene conversion drops to 86% after 6 h of time on stream). The system calcined at 1100 °C presented lower but stable conversion of toluene (with mean value of 62%) during 6.5 h of time on stream. The lower conversion seems to be a logical consequence of its lower reducibility—only 1.3 wt% Ni⁰ is obtained after reduction. Nevertheless, if those two systems are compared in terms of toluene conversion divided by the quantity of reduced Ni, the N1100 catalyst presents slightly higher activity. On the other hand the Ni/olivine system calcined at 1400 °C does not contain reducible Ni species, as shown by TPR. Its activity (24% of toluene conversion) is thus uniquely due to the presence of reduced iron species (3.2 wt% Fe⁰).

It appears that a minimal calcination temperature of 1100 °C is required to assure strong nickel–olivine interaction,

manifested in the formation of NiO–MgO solid solution, and avoid carbon deposition and catalyst deactivation. In order to confirm this sentence, catalysts calcined at 400 °C (N400) and 1100 °C (N1100) were tested in steam reforming of toluene for a S/C ratio of 2.3 and a catalyst mass (w_{cat}) of 200 mg at a much lower temperature (560 °C) than the operation temperature (800 °C) to favor carbon formation and permit a better comparison of the catalysts performances by amplification of the phenomenon.

Results confirm that catalytic activity decreases with increasing calcination temperature. In fact, toluene conversion is about 65% for N400 and 29% for N1100 in these conditions. However, the catalyst N400 is rapidly deactivated, as observed by a decrease in toluene conversion of about 45% after a time on stream of 7 h. At the same time, no decrease in N1100 activity was observed. The reason of this deactivation will be explained further by carbon deposition studied by TPO.

3.1.5. Nickel content effect

Preliminary results demonstrated that, with 200 mg of catalyst (precursor = nitrate, calcination temperature = 1100 °C), steam toluene conversion increased from 12 to 36% at 560 °C when nickel content increased from 1.5 to 5.7 wt%. However, when performing tests at a constant metal amount (Table 2), conversion was the same at 800 °C even when the nominal percentage of metal increased, clearly indicating that the nature of the active species does not change with nickel content. This could be explained by the particular interaction previously defined between nickel and the support observed for systems calcined at 1100 °C with all nickel contents studied [30,32].

The Ni/olivine catalysts calcined at 1100 °C contain a significant quantity of iron (2.4 wt% of Fe⁰ obtained by reduction in TPR conditions) in comparison to the quantity of nickel. As iron is a favorable metal for the water gas shift reaction, we expected an influence of iron to nickel ratio on CO to CO₂ ratio. However, this latter ratio remained unchanged for all iron/nickel ratios. This suggests that the kinetics of the water gas shift (WGS) reaction is much faster than reforming reactions, and that it is impossible to see the influence of nickel content on CO and CO₂ selectivities.

3.2. Operating parameters effect

In order to study the effect of operating parameters, we performed toluene steam reforming with the Ni/olivine catalyst N1100 (3.9 wt% Ni from nitrate calcined at 1100 °C) as a function of reaction temperature, S/C ratio and space-time. A comparison with results obtained at thermodynamic equilibrium is given.

3.2.1. Reaction temperature effect

Tests of steam reforming of toluene were performed in a temperature range of 560–850 °C for a S/C ratio of 2.3 and space-time ($w_{\text{cat}}/F_{\text{toluene}}$) at 25 °C of 9 kg_{cat} h m⁻³. No catalyst deactivation was observed after 7 h of time on stream.

We distinguished two temperature zones (Table 3). Up to 650 °C, toluene conversion and hydrogen yield increased with

Table 3

Reaction temperature effect on toluene conversion, carbon containing products selectivities, hydrogen yield and H₂/CO molar ratio during toluene steam reforming for N1100 catalyst (S/C = 2.3; time on stream = 7 h; $w_{\text{cat}}/F_{\text{toluene}} = 9$ kg_{cat} h m⁻³ at 25 °C)

Reaction temperature (°C)	560	600	650	750	850
Conversion (%)	29	74	100	100	100
CO	47	46	59	59	69
Selectivities (%)					
CO ₂	50	52	41	41	31
CH ₄	<1	<1	–	–	–
C ₆ H ₆	2	1	–	–	–
Polyaromatics	1	1	–	–	–
H ₂ yield (%)	32	73	84	80	78
H ₂ /CO ratio	5.1	5.0	4.2	3.6	3.3

reaction temperature. Benzene and polyaromatic compounds (2–3%) were observed in the products in addition to CO and CO₂. Above 650 °C, total toluene conversion to H₂, CO and CO₂ was obtained. Between 750 and 850 °C, we can note a decrease in hydrogen yield associated with a decrease in CO₂ and an increase in CO. The evolution of these results is due to a more important participation of the reverse water gas shift reaction (Eq. (6)), which is thermodynamically favorable at high temperatures.

Comparison of our results with the thermodynamic equilibrium curves (Fig. 3) revealed a complete agreement above 650 °C. Below this temperature, toluene steam reforming is governed by kinetics. Both thermodynamic equilibrium curve and our results (not shown in Fig. 3) give the benzene selectivity near to zero.

Results can be compared to those obtained with olivine alone. The latter shows almost no activity (<5%) until 750 °C, and moderate (37% at 850 °C) and weaker activity than with N1100 catalyst at 560 °C. For olivine, additionally to CO, CO₂ and H₂, significant selectivities towards methane (2%), benzene (6%) and polyaromatics (14%) are observed. Devi et al. [17] have also observed high benzene selectivity with olivine. These results illustrate the importance of nickel in the efficiency of catalyst during tar reforming.

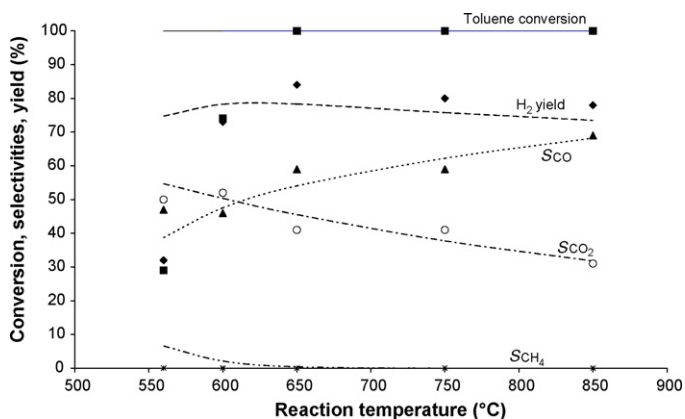


Fig. 3. Comparison of toluene steam reforming (toluene conversion, carbon containing product selectivities, and hydrogen yield) between our results with the N1100 catalyst (points) and thermodynamic equilibrium (lines).

We can also note that the H_2/CO ratio (Table 3) decreased progressively with an increase in reaction temperature. This can again be related to the temperature dependence of the water gas shift reaction (Eq. (6)). The high value of H_2/CO ratio at low temperatures can be also connected to higher carbon formation, leading to CO consumption during Boudouard reaction.

3.2.2. S/C ratio effect

Study of the effect of the S/C ratio on toluene steam reforming was performed for N1100 catalyst at 560 °C. In the range of S/C ratios studied, from 1.1 to 3.4, no influence on toluene conversion was observed. These results are in agreement with the results obtained by Simell et al. [14] and by Garcia and Hüttinger [37] who studied steam reforming of benzene over calcined dolomite and naphthalene steam reforming over CaO, respectively, and found that the reaction rate of hydrocarbon is independent of steam partial pressure with stoichiometric and higher ratios of steam/hydrocarbon. The latter assumed that this was due to saturation of the catalyst surface by steam at steam/naphthalene ratios higher than 10. This explanation could be also validated for the Ni/olivine catalyst in which nickel is in direct contact with MgO, significantly enhancing steam adsorption. In the same range of S/C ratios, no variation of CO and CO₂ selectivities was observed because of the products dilution and the low toluene conversion obtained.

3.2.3. Space-time effect

Catalyst (particle size 250–315 μm) was mixed with the appropriate amount of silicon carbide (the same particle size as catalyst) to a constant length of catalyst + SiC bed (4 mm).

The space-time was varied by changing the amount of catalyst, at a given feed rate, with constant feed composition and temperature. A similar series of measurements was performed for temperatures ranging from 560 to 800 °C. The data collected for toluene conversion as a function of space-time, was used to develop the kinetic equation for toluene steam reforming. Comparison of these results suggests that raising the temperature from 560 to 800 °C allows reduction of space-time about two orders of magnitude at the same conversion.

Fig. 4 shows the influence of space-time on selectivity of carbon containing products at different temperatures. The selectivities obtained at low space-times permitted identification of the primary reaction products: CO and benzene. For all temperatures studied, an increase in space-time led to an increase in CO₂ selectivity, formed from CO via the water gas shift reaction.

3.3. Kinetic parameters study

3.3.1. External and internal diffusion limitations

It is of interest to conduct kinetic studies in the conditions where heat and mass transfer resistances are absent. Also, it is necessary to obtain kinetic data using a catalyst bed where fluid channeling and back mixing are absent. According to the literature [38,39], using these conditions for collecting accurate intrinsic kinetic data can be achieved by employing catalyst in

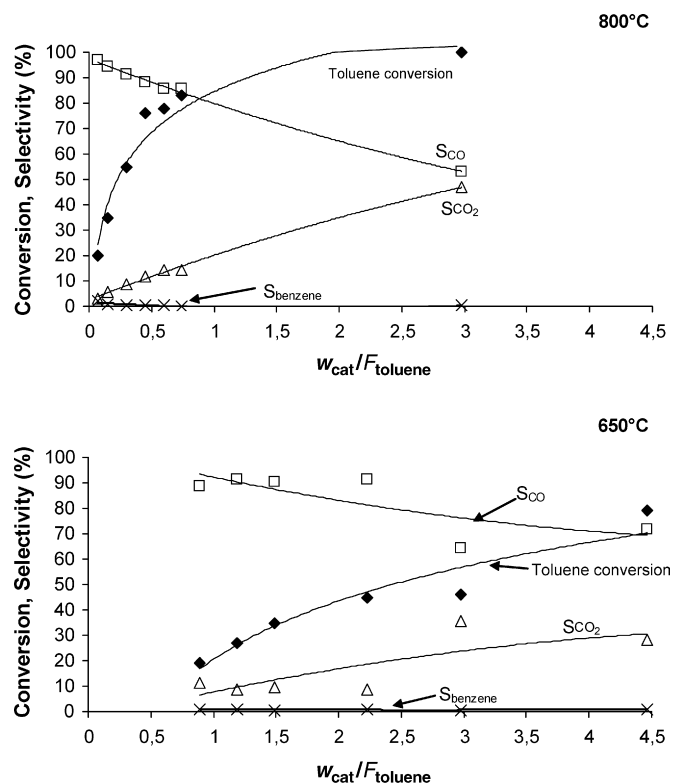


Fig. 4. Influence of space-time on toluene conversion and selectivity to carbon containing products during toluene steam reforming at different temperatures (N1100 catalyst).

the appropriate average size range, appropriate ranges of feed velocity and residence time, as well as other criteria necessary for plug flow and isothermal behavior in the reactor. The appropriate values of these variables were obtained by the study of the external (film) and internal (pore) diffusion effect on toluene conversion. It can be concluded that external diffusion does not contribute to the toluene decomposition rates, observed for a total feed flow rate, higher than $0.04 \text{ m}^3 \text{ h}^{-1}$ (higher than $0.012 \text{ m}^3 \text{ h}^{-1}$ at 25 °C), and that the effect of internal diffusion was negligible for particles sizes lower than 315 μm.

The studies of tar model compound (toluene) decomposition kinetics described below were carried out in conditions free of mass and heat transfer limitations.

3.3.2. Kinetic model

The high dilution of reactants assures a limited gas expansion (7–8 vol.%) in the reactor which can be considered as a plug-flow (constant flow-rate through it). According to the aforementioned experimental results and literature data showing no influence of water concentration on conversion of toluene (X_c) for S/C values higher than stoichiometric ratio (2), we have assumed that the power-law type general equation for the disappearance rate of tar in a binary reaction with H₂O can be expressed as a pseudo-order reaction with respect to only toluene concentration.

The decomposition rate of tar can be assumed to be first-order, as widely accepted in the literature data [27,37,40–42].

The first order rate constants can be calculated according to the following equation (Eq. (7)), derived from an integral plug flow reactor model [43].

$$k' (\text{m}^3 \text{kg}^{-1} \text{h}^{-1}) = \frac{-\ln(1 - X_c)}{\tau} \quad (8)$$

Temperature dependence on the rate constant was determined by the Arrhenius equation, from which the activation energy (E_a) and pre-exponential factor ($A(k')$) of the rate constant can be calculated.

3.3.3. Kinetic parameter values

Apparent first order kinetic parameters for steam reforming reactions of toluene on N1100 were estimated. Table 4 presents the determined parameter values.

These values are in concordance with values reported by Jess [44] for benzene decomposition on a commercial nickel catalyst (Ni/MgO, G117-Sud Chemie AG), performed in a gas atmosphere containing H_2O and H_2 (196 kJ mol^{-1}). Comparatively, Taralas et al. [45] reported higher activation energy values of 356 and 250 kJ mol^{-1} for thermal destruction of toluene in gas atmospheres containing H_2O in the presence of O_2 or H_2 , respectively. This comparison demonstrates the efficiency of the Ni/olivine catalyst in toluene steam reforming.

On the other hand, the activation energy value reported by Devi et al. [46] for the reforming of naphthalene on pretreated olivine was similar (187 kJ mol^{-1}) to the values we found for the reforming of toluene on the Ni/olivine catalyst. Likewise, Aznar et al. [47] observed a value of 58 kJ mol^{-1} for tar steam reforming on commercial nickel catalysts. In fact, it has been demonstrated [27] that when a single first-order expression approximates an independent overlapping set, first-order reactions (case of the overall tar removal), the E_{app} has a tendency to favor the lower value in the set. This approximation leads to a difficult comparison of the data from tar or model compound studies.

3.4. Characterization after steam reforming of toluene

In order to study the final state of Ni/olivine catalysts after toluene steam reforming and to explain the reasons of their stability or eventual deactivation, X-ray diffraction (XRD), Mössbauer spectroscopy, transmission electron microscopy (TEM) and temperature programmed oxidation (TPO) were performed. These techniques have allowed us to estimate an eventual loss of active phase (Ni), identify the nature of present phases and the state of nickel and iron and quantify the carbonaceous deposit. In order to prevent this phenomenon, we

examined the influence of preparation and operating parameters. In fact, the main constraint in tar reforming was catalyst deactivation caused by coke deposition.

3.4.1. Crystalline phases

The X-ray diffractograms of N1100 catalyst after steam reforming of toluene (6 h) at different temperatures were similar to those obtained after reduction of the catalyst [32]. Additionally to the unchanged diffraction pattern of the olivine support, the main diffraction line that could be attributed to nickel, iron or Ni-Fe alloys, was observed for all used catalysts, and its intensity increased with the reaction temperature as nickel became more reduced at higher temperatures. The mean metallic particle size calculated from the peak widening was 20 nm. In the catalysts used, the intensity of the main reflections of NiO and $\alpha\text{-Fe}_2\text{O}_3$ diminished and the spinel iron oxide phase was partially reduced. The reduction degree increased with an increase in the reaction temperature.

3.4.2. Nickel and iron distribution

The catalyst N1100 was examined by Mössbauer spectroscopy after toluene steam reforming at 800°C (Fig. 5). Five Fe containing components (olivine, $\alpha\text{-Fe}_2\text{O}_3$, spinel phase, carbides and Ni-Fe alloys) may be characterized and their distribution is presented in Table 5. The results come from curve fitting and the values of relative percentage of iron in different phases should be considered as semi quantitative. 14% of total iron was present in the form of carbide and 8% in the form of metallic iron—together 22% of total iron that represents about 1.5 wt% Fe in the catalyst. This value is in good agreement with previous results obtained from reducibility study of Ni/olivine calcined at 1100°C [32],

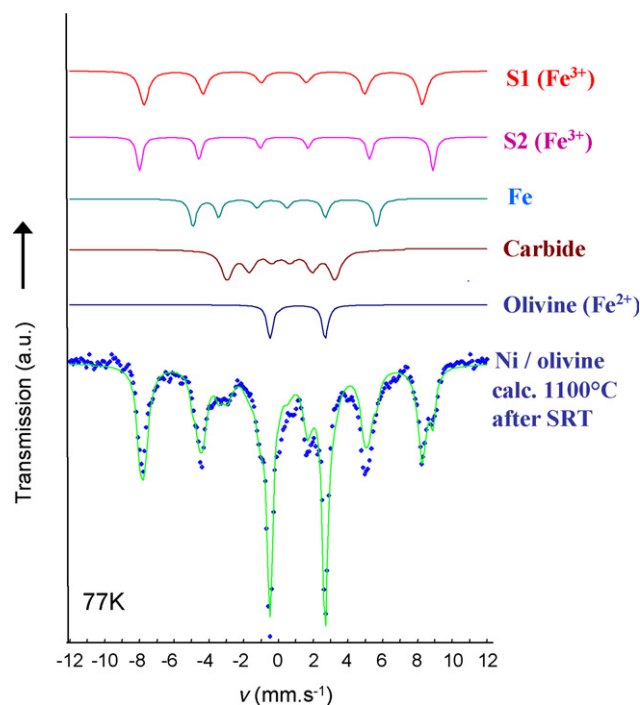


Fig. 5. ^{57}Fe Mossbauer spectra at -196°C (77 K) of the N1100 catalyst after steam reforming of toluene (800°C); the sub-spectra of the five components are indicated at the top.

Table 4
Estimates of the kinetic parameters for the first order toluene decomposition rate on N1100 catalyst

Parameter	Estimated value
$k' (T_r) (\text{m}^3 (\text{kg}_{\text{cat}} \text{h})^{-1})$	1896 (800°C)
$A (k') (\text{m}^3 (\text{kg}_{\text{cat}} \text{h})^{-1})$	3.14×10^{13}
$E_a (\text{kJ mol}^{-1})$	196

Table 5

Iron distribution obtained by Mössbauer spectroscopy for N1100 after steam reforming of toluene (800 °C, S/C = 2.3)

Iron type	Molar percentage (%)
Fe ²⁺ (olivine)	30
Fe ³⁺ (α -Fe ₂ O ₃)	11
Fe ³⁺ (spinel)	37
Fe ³⁺ (carbides)	14
Fe ⁰ (Ni–Fe alloys)	8

which give a quantity of metallic iron, obtained after reduction, of 31% of total iron that represents about 2.1 wt% of iron present in the catalyst.

The reduction of iron is important for the formation of Ni–Fe alloys and because iron metal can act as hydrocarbons reforming catalyst as demonstrated by Matsuoka et al. [48].

3.4.3. Carbon deposit study

TEM characterization of the catalyst after reactivity testing allowed us to determine the nature and morphology of the carbon deposits. Filaments (carbon nanotubes) grew on Ni–Fe particles with a variable Ni/Fe ratio and mean size of 50–200 nm (Fig. 6a). As shown in Fig. 6a and b, Ni–Fe particles composition can vary from rich in nickel to rich in iron.

Total carbon content in used catalysts was determined by TPO experiments and confirmed by elemental analysis of carbon. With TPO, two peaks of CO₂ can be seen. The low temperature peak, at about 380 °C, can be attributed to the oxidation of surface metal carbide [49]. The peak at 650 °C was associated with the graphitic carbon in the form of carbon filaments and nanotubes (TEM). Similar TPO profiles were obtained for catalysts prepared with different precursors (N1100, C1100 and A1100), indicating that the nickel precursor has no effect on carbon deposition during toluene steam reforming at 800 °C with a S/C ratio of 2.3. No soluble components were detected by extraction with C₂S followed by GC analysis.

3.4.3.1. Calcination temperature effect. TPO for catalysts calcined at different temperatures (N900, N1100 and N1400) indicate that a very low carbon amount is formed on each

catalyst during toluene steam reforming at 800 °C with a S/C ratio of 2.3. The main difference was observed in the amount of carbides, which increased as calcination temperature decreased, and can be related to the amount of metal phase available for reduction [34]. As discussed previously in the activity study, N900 leads to the formation of a greater amount of carbon than N1100.

The conditions promoting carbon formation have been chosen for better understanding of carbon deposition resistance of different catalysts. The following studies of carbon formation were carried out at 560 °C, a temperature at which this reaction is thermodynamically favorable.

TPO obtained for catalyst N400 after steam reforming of toluene at 560 °C was compared to that obtained for catalyst N1100, in the same conditions, in Fig. 7. About 10 times more carbon (850 compared to 80 $\mu\text{g}/(\text{g}_{\text{cat}} \text{h } C_{\text{conv}})$), usually observed in carbon filament species, was formed on catalyst N400 as expected according to the behavior of catalyst deactivation. This carbon deposition is associated with the presence of free NiO (reducible at ~ 400 °C) on the olivine surface of this sample.

As previously observed by TPR, free NiO was also present on the catalyst N900 what implies the formation of carbon and explains the deactivation of the catalyst N900. That suggests an optimal calcination temperature of 1100 °C.

3.4.3.2. Nickel content effect. TPO profiles of catalysts with different nickel contents were obtained after toluene steam reforming at 560 °C (Fig. 8). Carbon deposit amount was proportional to nickel content in the catalyst. This behavior was observed for both carbon types.

3.4.3.3. S/C ratio effect. Although water content had no influence on toluene conversion and carbon containing product selectivities, it affected the amount of carbon deposited on the catalyst (Fig. 9). The amount of carbon formed on the Ni/olivine catalyst decreased from 180 to 30 $\mu\text{g}/(\text{g}_{\text{cat}} \text{h } C_{\text{conv}})$, with an increasing S/C molar ratio from 1.1 to 3.4. The peak, at 660 °C, increased significantly with a decreasing S/C ratio. However, the peak, at 380 °C, remained practically unchanged for all S/C ratios, suggesting that the amount of carbides is

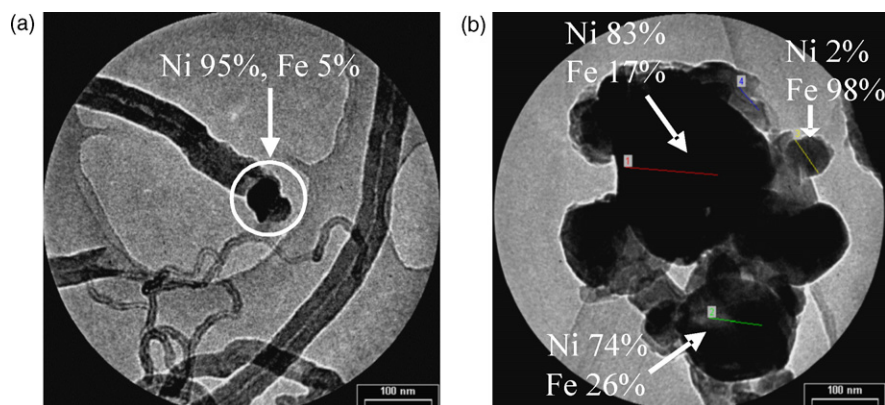


Fig. 6. TEM micrographs (a) carbon filaments formed on the N1100 catalyst during steam reforming of toluene at 560 °C and (b) Ni–Fe particles after reaction at 800 °C (S/C = 2.3).

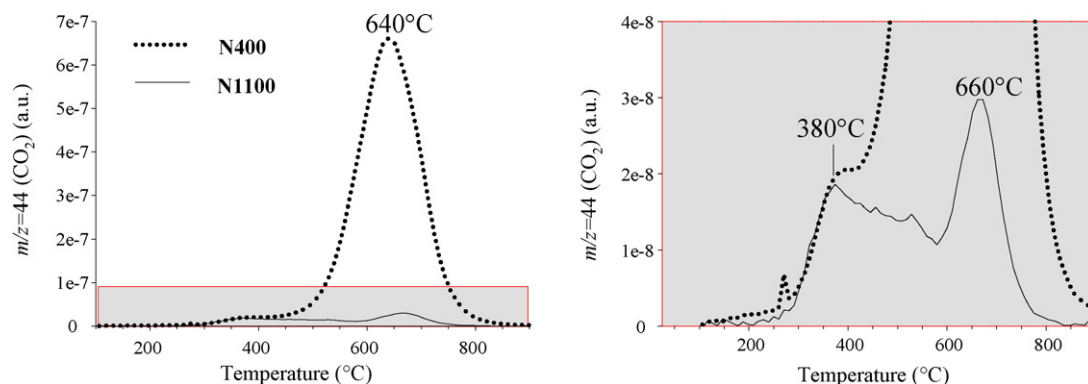


Fig. 7. TPO profiles of catalysts N400 and N1100 tested in steam reforming of toluene (560 °C; S/C = 2.3).

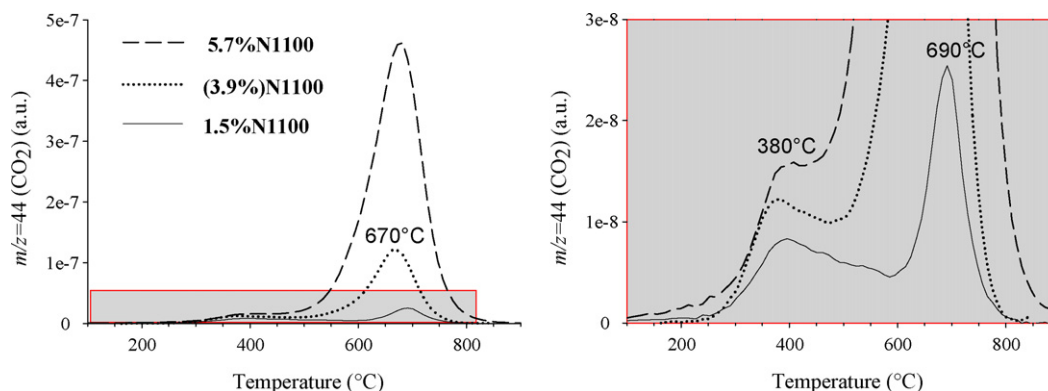


Fig. 8. TPO profiles of catalysts with different nickel content tested in steam reforming of toluene (560 °C; S/C = 2.3).

independent of steam content. Higher steam content, however, significantly decreased the amount of filamentous carbon.

3.4.3.4. Reaction temperature effect. The temperature used during toluene reforming influenced the amount and distribution of both types of carbon (Fig. 10). The total amount of carbon formed on N1100 catalyst, at S/C = 2.3, decreased from 80 to 3 $\mu\text{g}/(\text{g}_{\text{cat}} \text{h } C_{\text{conv}})$ with an increasing reaction temperature from 560 to 800 °C. Taking into account the total carbon converted during the test period, it represents the selectivities towards carbon formation of 1.4% at 560 °C and <0.1% at 800 °C. For N1100 catalyst, after reaction at 560 and 750 °C, a decrease in both types of carbon (or total amount of carbon) was observed with increasing temperature. Practically only carbide was detected after reaction at 800 °C.

3.4.3.5. Catalyst stability. The optimized catalyst (N1100) was stable during 6.5 h of time on stream and catalyst deactivation observed on N900 sample was associated to a higher formation of carbon as explained previously.

It is important to note that no catalyst reduction-activation is needed before reactivity tests although Ni^0 sites are required for hydrocarbons reforming. In fact, catalyst is partially reduced in-situ by reactant stream and this reduced state is sufficient to start the reforming reaction. This one leads to the formation of $\text{CO} + \text{H}_2$ and then to a more reducing conditions which maintains a sufficient level of catalyst reduction.

So, in our test conditions (S/C varies between 1.1 and 3.4), no catalyst deactivation is observed related to a partial oxidation of the catalyst by steam. On the other hand, Corella et al. [50] have reported that our optimized Ni/olivine catalyst is

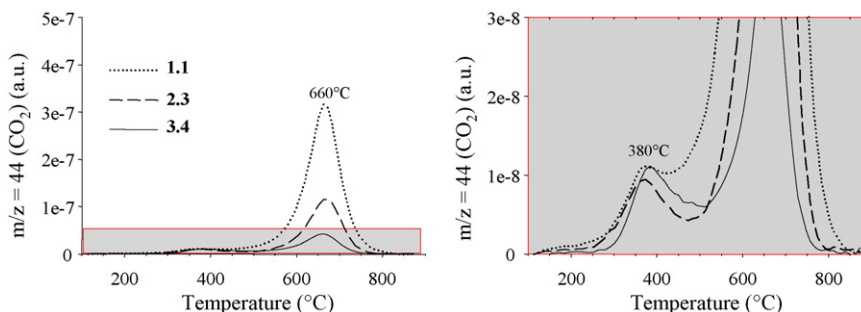


Fig. 9. TPO for N1100 catalyst after steam reforming of toluene at 560 °C with different S/C ratios.

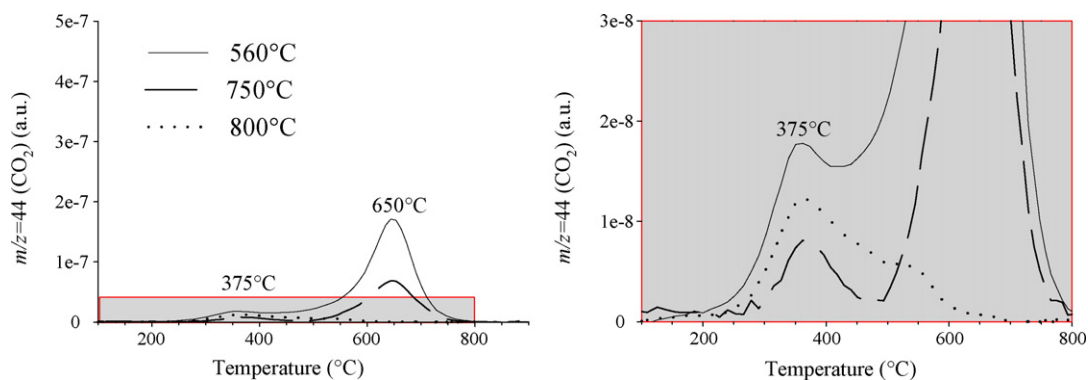


Fig. 10. TPO profiles of N1100 catalyst tested in steam reforming of toluene at different temperatures.

not very active for tar elimination in biomass gasification with air. Their results are probably related to the catalyst unreduced state in highly oxidizing conditions of air gasification.

On the other hand, this optimized catalyst was tested in steam reforming of methane in fixed bed reactor with a gas mixture model based on the composition of the outlet stream of the biomass gasifier developed at the University of Vienna [51] and with various water contents. The results, in good agreement to those obtained by Hofbauer et al. [51], have permitted to determine optimal water content of 35 vol.% to prevent catalyst deactivation. For lower water content (21 vol.%), catalyst deactivation could be due to carbon formation. For higher water content (50 vol.%), catalyst deactivation could be due to catalyst oxidation.

Finally, the stability of the N1100 catalyst in the model conditions of steam reforming of toluene in a fixed bed micro-reactor is in excellent agreement with the previous results of biomass steam gasification in a dual fluidized bed gasifier where this catalyst was used as bed material [33]. In that 100 kWth pilot plant the performance of the catalyst over 30 h showed no loss of reactivity for cracking tars and no deactivation by common catalyst poisons (sulfur, chlorine, and alkali metals). The reason of this stability lies in the strong metal-support interactions [31,32], which provide resistance against attrition, carbon formation and for repeated high temperature processing in oxidizing and reducing atmosphere during circulation between the fluidized beds.

3.4.3.6. Comparison with olivine. The two systems, Ni/olivine and initial olivine, have been compared after tests with a S/C ratio of 2.3. Better performance of Ni/olivine catalyst than initial olivine alone was illustrated by analyzing carbon content in spent catalyst as a function of toluene conversion. At 850 °C, Ni/olivine led to total toluene conversion and carbon content comparable to that obtained on initial olivine after only 37% toluene conversion [52].

Low carbon deposition on the Ni/olivine catalyst can be explained on the basis of a simplified mechanism for catalytic tar reforming [53], which can be described as follows. First, the dealkylation of the methyl group of toluene occurs and leads to the formation of benzene as primary product. The methyl groups are adsorbed onto a metal site then reformed to CO + H₂. Hydrogen can then hydrogenate the aromatic rings to

form saturated cyclic ring which can break down easily in hydrocarbon fragments which are transformed into CO + H₂. Water is also dissociatively adsorbed onto the oxide support, hydroxylating the surface. At the appropriate temperature, the OH radicals migrate to the metal sites, leading to oxidation of the intermediate hydrocarbon fragments and surface carbon to CO + H₂. The presence of MgO at the interface between olivine and nickel, demonstrated previously [31,32], enabled steam adsorption and increased surface carbon gasification rates [53].

On the other hand, nickel dilution effect, associated with iron–nickel alloy (particle size of 50–200 nm) formation, observed by TEM and Mössbauer spectroscopy [32], can explain low carbon deposition, as previously demonstrated in our laboratory [54].

4. Conclusions

The efficiency of the Ni/olivine catalyst in tar removal from gasification gas, demonstrated previously [33], was confirmed by using a model of toluene steam reforming.

The results concerning the effect of preparation parameters (nickel salt, calcination temperature, and nickel content) on catalyst activity are in good agreement with those previously obtained in studies of methane reforming [30]. Taking into account the activity of various catalysts in toluene steam reforming and the amount of carbon deposited after such catalytic tests, optimized catalyst was prepared with nitrate nickel and calcined at 1100 °C. The nature of the active species did not change when nickel content was varied between 1.5 and 5.7 wt%. So N1100 activity increased with nickel content, although the amount of carbon deposition (both carbon types) was also proportional to this parameter.

The study performed on this optimized catalyst, with 3.9 wt% of Ni, as a function of operating parameters (reaction temperature, S/C ratio and space-time) demonstrates that, for a reaction temperature higher than 650 °C, total toluene conversion is obtained and carbon formation is negligible. The main gaseous reaction products are H₂ and CO which are having proportions in good agreement with thermodynamic equilibrium. The total amount of carbon formed on the N1100 catalyst decreased with an increase in reaction temperature. Reducing space-time about two orders of magnitude, gave the same conversion when the temperature was raised from 560 to

800 °C. In the range of studied S/C ratios, from 1.1 to 3.4, no influence on toluene conversion or CO and CO₂ selectivities was observed, although the amount of carbon formed on the Ni/olivine catalyst decreased from 180 to 30 μg/(g_{cat} h C_{conv}). The catalyst stability resulting from resistance towards carbon formation can be explained on the base of the particular structure of the reduced catalyst which can be described as Ni–Fe/MgO/olivine system. Both factors – the presence of Ni–Fe alloys and basic MgO oxide – are beneficial for limiting carbon formation.

The importance of Ni/olivine catalyst was clearly demonstrated by the comparison with olivine alone: higher activity, higher selectivity to H₂ and CO, and lower carbon deposition.

The kinetic model proposes, as generally accepted, a zero order for water and an order one for toluene with activation energy of 196 kJ mol⁻¹, comparable to literature data, in which conditions were free of mass and heat transfer limitations.

Acknowledgements

The financial support of the E.U. under the contract ENK5-CT-2000-00314 is gratefully acknowledged. Authors thank to L. Bedel for his collaboration in the interpretation of Mössbauer spectra, Y. Zimmermann for transmission electron microscopy and a reviewer for his suggestion of mechanism.

References

- [1] H. Hofbauer, T. Fleck, G. Veronik, R. Rauch, H. Mackinger, E. Fercher, in: A.V. Bridgwater, D.G.B. Boocock (Eds.), *The FICFB-Gasification Process, Developments in Thermochemical Biomass Conversion*, Blackie, London, 1997, pp. 1016–1025.
- [2] R. Rauch, C. Pfeifer, K. Bosch, H. Hofbauer, D. Świerczyński, C. Courson, A. Kiennemann, in: A.V. Bridgwater, D.G.B. Boocock (Eds.), *Science in Thermal and Chemical Biomass Conversion*, 1, CPL Press, 2006, pp. 799–809.
- [3] A.V. Bridgwater, *Chem. Eng. J.* 91 (2003) 87.
- [4] T.A. Milne, N. Abatzoglou, R.J. Evans, *Biomass Gasifier 'Tars': their nature, formation and conversion*. NREL Technical Report (NREL/TP-570-25357), November 1998.
- [5] A.V. Bridgwater, *Fuel* 74 (1995) 631.
- [6] P.A. Simell, J.K. Leppälähti, J.B. Bredenberg, *Fuel* 71 (1992) 211.
- [7] I. Narvaez, A. Orio, M.P. Aznar, J. Corella, *Ind. Eng. Chem. Res.* 35 (1996) 2110.
- [8] G. Taralas, *Ind. Eng. Chem. Res.* 35 (1996) 2121.
- [9] J. Delgado, M.P. Aznar, J. Corella, *Ind. Eng. Chem. Res.* 36 (1997) 1535.
- [10] P. Perez, M.P. Aznar, M.A. Caballero, J. Gil, J.A. Martin, J. Corella, *Energy Fuels* 11 (1997) 1194.
- [11] P.A. Simell, N.A.K. Hakala, H.E. Haario, A.O.I. Krause, *Ind. Eng. Chem. Res.* 36 (1997) 42.
- [12] P.A. Simell, J.O. Hepola, A.O.I. Krause, *Fuel* 76 (1997) 1117.
- [13] J. Gil, M.A. Caballero, J.A. Martin, M.P. Aznar, J. Corella, *Ind. Eng. Chem. Res.* 38 (1999) 4226.
- [14] P.A. Simell, E.K. Hirvensalo, V.T. Smolander, A.O.I. Krause, *Ind. Eng. Chem. Res.* 38 (1999) 1250.
- [15] S. Rapagnà, N. Jand, A. Kiennemann, P.U. Foscolo, *Biomass Bioenergy* 19 (2000) 187.
- [16] J. Corella, A. Orio, J.M. Toledo, *Energy Fuels* 13 (1999) 702.
- [17] L. Devi, K.J. Ptasiński, F.J.J.G. Janssen, S.V.B. van Paasen, P.C.A. Bergman, J.H.A. Kiel, *Renewable Energy* 30 (2005) 565.
- [18] T. Furusawa, A. Tsutsumi, *Appl. Catal., A* 278 (2005) 207.
- [19] P.A. Simell, E. Kurkela, P. Ståhlberg, J. Hepola, *Catal. Today* 27 (1996) 55.
- [20] D.N. Bangala, N. Abatzoglou, J.P. Martin, E. Chornet, *Ind. Eng. Chem. Res.* 36 (1997) 4184.
- [21] T. Wang, J. Chang, X. Cui, Q. Zhang, F. Yan, *Fuel Process. Technol.* 87 (2006) 421.
- [22] D. Dayton, A review of the literature on catalytic biomass tar destruction, NREL, Golden, CO, USA, (NREL/TP-510-32815), 2002.
- [23] J. Corella, J.M. Toledo, R. Padilla, *Ind. Eng. Chem. Res.* 44 (2005) 2036.
- [24] K. Tomishige, Y.G. Chen, K. Fujimoto, *J. Catal.* 181 (1999) 91.
- [25] S. Czernik, R. French, C. Feik, E. Chornet, *Ind. Eng. Chem. Res.* 41 (2002) 4209.
- [26] M.A. Caballero, J. Corella, M.P. Aznar, J. Gil, *Ind. Eng. Chem. Res.* 39 (2000) 1143.
- [27] J. Corella, J.M. Toledo, M.P. Aznar, *Ind. Eng. Chem. Res.* 41 (2002) 3351.
- [28] K.A. Magrini-Bair, S. Czernik, R. French, Y.O. Parent, E. Chornet, D.C. Dayton, C. Feik, R. Bain, *Appl. Catal. A* 318 (2007) 199.
- [29] C. Courson, C. Petit, A. Kiennemann, P.U. Foscolo, S. Rapagnà, M. Matera, *European Patent PCT/FR01/01547* (2001).
- [30] C. Courson, L. Udron, D. Świerczyński, C. Petit, A. Kiennemann, *Catal. Today* 76 (2002) 75.
- [31] D. Świerczyński, C. Courson, J. Guille, A. Kiennemann, *J. Phys. IV* 118 (2004) 385.
- [32] D. Świerczyński, C. Courson, L. Bedel, A. Kiennemann, J. Guille, *Chem. Mater.* 18 (2006) 4025.
- [33] C. Pfeifer, R. Rauch, H. Hofbauer, D. Świerczyński, C. Courson, A. Kiennemann, in: A.V. Bridgwater, D.G.B. Boocock (Eds.), *Science in Thermal and Chemical Biomass Conversion*, 1, CPL Press, 2006, pp. 677–690.
- [34] D. Świerczyński, C. Courson, L. Bedel, A. Kiennemann, S. Vilminot, *Chem. Mater.* 18 (2006) 897.
- [35] M.D. Brown, E.G. Baker, L.K. Mudge, *Biomass* 11 (1986) 255.
- [36] M. Serra, P. Salagre, Y. Cesteros, F. Medina, J.E. Sueiras, *Solid State Ionics* 134 (2000) 229.
- [37] X.A. Garcia, K.J. Hüttinger, *Erdöl Kohle, Erdgas. Petrochem.* 43 (1990) 273.
- [38] H.F. Rase, *Chemical Reactor design for Processes Plants*, Wiley, New York, 1987, pp. 185–188 and 195–259.
- [39] G.F. Froment, K.B. Bishoff, *Chemical Reactor Analysis and Design*, Wiley, New York, 1979.
- [40] G. Taralas, V. Vassilatos, K. Sjöstrom, J. Delgado, *Can. J. Chem. Eng.* 69 (1991) 1413.
- [41] B.G. Espenas, L. Waldenheim, *Advanced gasification of biomass: upgrading of the crude gasification product gas for electricity and heat generation*. Termiska Processer AB (TPS 96/17), Sweden, 1996.
- [42] O.S.L. Bruinsma, R.S. Geertsma, P. Bank, J.A. Moulijn, *Fuel* 67 (1988) 327.
- [43] O. Levenspiel, *Chemical Reaction Engineering*, 3rd ed., Wiley, New York, 1972, pp. 500–519.
- [44] A. Jess, *Chem. Eng. Process.* 35 (1996) 487.
- [45] G. Taralas, M.G. Kontominas, X. Katatsios, *Energy Fuels* 17 (2003) 329.
- [46] L. Devi, K.J. Ptasiński, F.J.J.G. Janssen, *Fuel Process. Technol.* 86 (2005) 707.
- [47] M.P. Aznar, M.A. Caballero, J. Gil, J.A. Martin, J. Corella, *Ind. Eng. Chem. Res.* 37 (1998) 2668.
- [48] K. Matsuoka, T. Shimbori, K. Kuramoto, H. Hatano, Y. Suzuki, *Energy Fuel* 20 (2006) 2727.
- [49] H.M. Swaan, V.C.H. Kroll, G.A. Martin, C. Mirodatos, *Catal. Today* 21 (1994) 571.
- [50] J. Corella, J.M. Toledo, R. Padilla, *Energy Fuels* 18 (2004) 713.
- [51] H. Hofbauer, R. Rauch, *Progress in thermochemical biomass conversion conference, Innsbruck, Austria (09/2000)*.
- [52] D. Świerczyński, C. Courson, A. Kiennemann, *Récents Progrès en Génie des Procédés*, No. 92 – 2005, Ed. SFGP, Paris, France.
- [53] L. Garcia, R. French, S. Czernik, E. Chornet, *Appl. Catal., A* 201 (2000) 225.
- [54] H. Provendier, C. Petit, A. Kiennemann, *A.C.R. Acad. Sci., Ser. IIC: Chim.* 4 (2001) 57.